J|A|C|S
ARTICLES
Published on Web 02/06/2004

An Example of O_2 Binding in a Cobalt(II) Corrole System and High-Valent Cobalt−Cyano and Cobalt−Alkynyl Complexes

Bobby Ramdhanie,[†] Joshua Telser,[‡] Andrea Caneschi,[§] Lev N. Zakharov,[||] Arnold L. Rheingold,[||] and David P. Goldberg*[,†]

Contribution from the Department of Chemistry, Johns Hopkins University, 3400 North Charles Street, Baltimore, Maryland 21218, Chemistry Program, Roosevelt University, Chicago, Illinois 60605, Dipartimento di Chimica e UdR INSTM di Firenze, Polo Scientifico, Via della Lastruccia 3, 50019 Sesto Fiorentino, Italy, and Department of Chemistry and Biochemistry, University of California, San Diego, 9500 Gilman Drive, La Jolla, California 92093

Received June 30, 2003; E-mail: dpg@jhu.edu

Abstract: The novel cobalt corrolazine (Cz) complexes $(TBP)_8CzCoCN$ (**1**) and $(TBP)_8CzCo(CCSiPh_3)$ (**2**) have been synthesized and examined in light of the recent intense interest regarding the role of corrole ligands in stabilizing high oxidation states. In the case of **2**, the molecular structure has been determined by X-ray crystallography, revealing a short Co−C distance of 1.831(4) Å and an intermolecular π-stacking interaction between Cz ring planes, and this structure has been analyzed in regards to the electronic configuration. By a combination of spectroscopic techniques it has been shown that **1** is best described as a cobalt(III)−π-cation-radical complex, whereas **2** is likely best represented as the resonance hybrid $(Cz)Co^{IV}(CCSiPh_3) \leftrightarrow (Cz^{+\bullet})Co^{III}(CCSiPh_3)$. The reduced cobalt(II) complex, $[(TBP)_8CzCo^{II}(py)]^-$, has been generated in situ and shown to bind dioxygen at low temperature to give $[(TBP)_8CzCo^{III}(py)(O_2)]^-$. For the reduced complex $[(TBP)_8CzCo^{II}(py)]^-$, the EPR spectrum in frozen solution is indicative of a low-spin cobalt(II) complex with a d_{z^2} ground state. Exposure of $[(TBP)_8CzCo^{II}(py)]^-$ to O_2 leads to the reversible formation of the cobalt(III)−superoxo complex $[(TBP)_8CzCo^{III}(py)(O_2)]^-$, which has been characterized by EPR spectroscopy. VT-EPR measurements show that the dioxygen adduct is stable up to $T \approx 240$ K. This work is the first observation, to our knowledge, of O_2 binding to a cobalt(II) corrole.

Introduction

The synthesis of corroles has a long history, but only in the past few years has there been an increase of interest in this class of porphyrinoid compounds.[1−4] Corroles are ring-contracted analogues of porphyrins that retain the tetrapyrrolic, 18-π-electron aromatic porphyrinoid nucleus. The stabilization of high oxidation states in transition metals is one of their most interesting features. The renewed interest in corroles has been spurred by important developments in the improved syntheses of *meso*-aryl-substituted corroles,[5−14] which in turn has led to many new discoveries in the synthesis, physical properties, and reactivity of transition metal−corrole complexes. A wide variety of intriguing high-valent transition metal complexes have been synthesized with corrole ligands, and certain metallocorroles have demonstrated catalytic activity (epoxidation, cyclopropanation).[15−19] Moreover, there has been a long-standing interest in corroles for their relevance to the chemistry of heme proteins as well as to the structurally related corrin cofactor found in vitamin B-12.

We have recently reported the synthesis of the first *triaza*-corrole, in which the *meso* carbon atoms have been replaced by nitrogen atoms, and we have given the trivial name "corrolazine (Cz)" to this new class of porphyrinoid com-

[†] Johns Hopkins University.
[‡] Roosevelt University.
[§] Dipartimento di Chimica e UdR INSTM di Firenze, Polo Scientifico.
[||] University of California.

(1) Sessler, J. L.; Weghorn, S. J. *Expanded, Contracted, & Isomeric Porphyrins*; Elsevier Science Inc.: New York, 1997; Vol. 15.
(2) Paolesse, R. In *The Porphyrin Handbook*; Kadish, K. M., Smith, K. M., Guilard, R., Eds.; Academic Press: New York, 2000; Vol. 2, pp 201−232.
(3) Erben, C.; Will, S.; Kadish, K. M. In *The Porphyrin Handbook*; Kadish, K. M., Smith, K. M., Guilard, R., Eds.; Academic Press: New York, 2000; Vol. 2, pp 233−300.
(4) Gryko, D. T. *Eur. J. Org. Chem.* **2002**, 1735−1743.
(5) Paolesse, R.; Licoccia, S.; Bandoli, G.; Dolmella, A.; Boschi, T. *Inorg. Chem.* **1994**, *33*, 1171−1176.
(6) Gross, Z.; Galili, N.; Saltsman, I. *Angew. Chem., Int. Ed.* **1999**, *38*, 1427−1429.
(7) Gross, Z.; Galili, N.; Simkhovich, L.; Saltsman, I.; Botoshansky, M.; Bläser, D.; Boese, R.; Goldberg, I. *Org. Lett.* **1999**, *1*, 599−602.
(8) Paolesse, R.; Jaquinod, L.; Nurco, D. J.; Mini, S.; Sagone, F.; Boschi, T.; Smith, K. M. *Chem. Commun.* **1999**, 1307−1308.
(9) Paolesse, R.; Nardis, S.; Sagone, F.; Khoury, R. G. *J. Org. Chem.* **2001**, *66*, 550−556.
(10) Gryko, D. T. *Chem. Commun.* **2000**, 2243−2244.
(11) Gryko, D. T.; Jadach, K. *J. Org. Chem.* **2001**, *66*, 4267−4275.
(12) Briñas, R. P.; Brückner, C. *Synlett* **2001**, 442−444.
(13) Asokan, C. V.; Smeets, S.; Dehaen, W. *Tetrahedron Lett.* **2001**, *42*, 4483−4485.
(14) Collman, J. P.; Decréau, R. A. *Tetrahedron Lett.* **2003**, *44*, 1207−1210.
(15) Gross, Z.; Simkhovich, L.; Galili, N. *Chem. Commun.* **1999**, 599−600.
(16) Gross, Z.; Golubkov, G.; Simkhovich, L. *Angew. Chem., Int. Ed.* **2000**, *39*, 4045−4047.
(17) Simkhovich, L.; Mahammed, A.; Goldberg, I.; Gross, Z. *Chem.-Eur. J.* **2001**, *7*, 1041−1055.
(18) Golubkov, G.; Bendix, J.; Gray, H. B.; Mahammed, A.; Goldberg, I.; DiBilio, A. J.; Gross, Z. *Angew. Chem., Int. Ed.* **2001**, *40*, 2132−2134.
(19) Mahammed, A.; Gray, H. B.; Meier-Callahan, A. E.; Gross, Z. *J. Am. Chem. Soc.* **2003**, *125*, 1162−1163.

pounds.[20] The synthesis of the metal-free triazacorrole $(TBP)_8CzH_3$ (TBP = 4-*tert*-butylphenyl) is easily accomplished in a few steps from commercially available reagents (six steps from 4-*tert*-butylbenzyl bromide) and is therefore of practical use as a ligand for transition metal chemistry. A series of cobalt complexes was recently prepared from $(TBP)_8CzH_3$.[21] The feasibility of stabilizing high-valent states with a corrolazine ligand has been demonstrated with the isolation and spectroscopic characterization of a stable manganese(V)−oxo complex, $(TBP)_8CzMn^V{\equiv}O$.[22,23] The analogous high-valent manganese corrole complexes $(tpfc)Mn^V{\equiv}O$[16] and $[(tpfc)Mn^V{\equiv}N]^-$[18] with 5,10,15-tris(pentafluorophenyl)corrole have been described previously, and another Mn^V−oxo complex has recently been prepared with a perfluorinated corrole.[24] In addition, the high-valent Mn^V−imido corrole complexes $(tpfc)Mn^V{=}NR$ (R = 2,4,6-trimethylphenyl; 2,4,6-trichlorophenyl) have recently been synthesized[25] and are the first examples of isolable Mn^V−terminal imido complexes. High-valent corrole complexes of other metals such as iron have been reported although, particularly with Fe, there is some debate about the noninnocence of the corrole and the true nature of the electronic configuration (e.g. $(corrole)Fe^{IV}L$ vs $(corrole^{+\bullet})Fe^{III}L$).[26−33] In cobalt−corrole chemistry, the only examples reported to date of formally high-valent systems are the σ-phenyl complexes (OEC)Co(Ph) and $[(OEC)Co(Ph)]ClO_4$ (OEC = octaethylcorrole) described by Kadish and Vogel.[34] Herein we describe the synthesis of two novel, formally high-valent, cobalt triazacorrole complexes with σ-carbon-bonded axial ligands, $(TBP)_8CzCo(CN)$ and $(TBP)_8CzCo(CCSiPh_3)$. These complexes have been examined for their structural and spectroscopic properties, and their electronic configurations are discussed in light of these data.

In addition to our interest in high oxidation state corrole complexes, we are also interested in the biomimetic chemistry of corroles and how they compare to their porphyrin counterparts. As part of these efforts we describe here the formation of a reduced cobalt(II) triazacorrole and its reactivity with dioxygen. It has been long established that cobalt(II) porphyrins will reversibly bind dioxygen in a manner similar to heme proteins (hemoglobin/myoglobin),[35,36] but to our knowledge O_2 binding to a cobalt(II) corrole complex of any type is unprecedented.[37] We have established that $[(TBP)_8CzCo^{II}(py)]^-$ exhibits reversible O_2 binding to give a Co^{III}−superoxo adduct at low temperature. In addition, it is demonstrated that the same complex under conditions of excess O_2 can generate the free superoxide anion.

Experimental Section

General Remarks. The starting material octa-*tert*-butylphenyl cobalt(III) corrolazine ($(TBP)_8CzCo^{III}$), was prepared as reported previously.[21] Reagents and solvents were purchased from commercial sources and were of reagent-grade quality. Tetrahydrofuran was distilled from Na/benzophenone under a nitrogen atmosphere. Preparation and handling of air-sensitive materials were carried out under an argon atmosphere using standard Schlenk techniques or in a Vacuum Atmospheres Company VAC-AV-3 inert atmosphere (<1 ppm O_2) drybox under nitrogen atmosphere. Solvents and solutions were deoxygenated by either repeated freeze−pump−thaw cycles or by direct bubbling of argon through the solution for 20−30 min. Dioxygen gas (ultrapure grade, 99.994%) was passed through a column of Drierite before being used. NMR spectra were measured on a Varian Unity FT-NMR instrument at 400 MHz (^1H) and 79 MHz (^{29}Si). All spectra were recorded in 5-mm o.d. NMR tubes, and chemical shifts were reported as δ values from standard solvent peaks. UV−vis spectral studies were carried out with a Hewlett-Packard 8453 diode array spectrometer equipped with HPChemstation software. Mass spectrometry was carried out using a Kratos SEQ MALDI-TOF mass spectrometer. IR spectra were obtained on a Perkin-Elmer RX I FT-IR Spectrometer. Electron paramagnetic resonance (EPR) spectra were obtained on a Bruker EMX EPR spectrometer controlled with a Bruker ER 041 X G microwave bridge. The EPR spectrometer was equipped with a continuous-flow liquid helium cryostat and ITC503 temperature controller made by Oxford Instruments, Inc. The field/frequency was calibrated by measuring the *g* value of DPPH. Elemental analyses were performed by Atlantic Microlab, Inc., Atlanta, GA.

Octa(*tert*-butylphenyl) Cobalt Corrolazine Cyanide $(TBP)_8CzCo(CN)$ (1): Method A. To a stirring solution of octa(*tert*-butylphenyl) cobalt corrolazine (250 mg, 0.177 mmol) in 50 mL of distilled pyridine was added an aqueous solution of sodium cyanide (4.0 g, 8.2 mmol). The solution was allowed to stir for 30 min at room temperature. The volatiles were removed under vacuum, and the resulting brown solid was redissolved in methylene chloride. Purification by silica gel chromatography (neat methylene chloride on silica) afforded a brown solid (180 mg 71%). $R_f = 0.4$. ^1H NMR (400 MHz, CD_2Cl_2): δ (ppm) 8.60−7.00 (br, 32H), 1.60−1.40 (br, 72H). UV−vis (CH_2Cl_2) λ_{max} [nm] ($\epsilon \times 10^{-4}$) 445 (4.6), 680 (1.6), 738 (1.5). IR: ν(CN) region (KBr) 2198, 2135 cm^{-1}. MALDI-TOF (negative ion mode): *m*/*z* (% intensity): 1440 (100, M + 1). Anal. Calcd for $C_{97}H_{104}N_8Co{\cdot}H_2O$: C, 79.86; H, 7.32; N, 7.68. Found: C, 79.60; H, 7.75; N, 7.90.

Method B. To a stirring solution of octa(*tert*-butylphenyl) cobalt corrolazine (250 mg, 0.177 mmol) in 50 mL of pyridine was added $(NH_4)_2Ce(NO_3)_6$ (1.0 g, 1.8 mmol) in EtOH (50 mL). The solution was allowed to stir for 30 min at room temperature. A solution of sodium cyanide (0.85 g, 17.3 mmol) in water (50 mL) was then added to the reaction mixture. After stirring for an additional 30 min, the solvents were removed under vacuum, and the resulting brown solid was redissolved into 100 mL of methylene chloride. The methylene chloride layer was washed with water (3 × 100 mL), dried over magnesium sulfate, and concentrated under vacuum. The brown solid was then redissolved into a minimal amount of methylene chloride and purified by silica gel chromatography (100 mg, 40.0%).

(20) Ramdhanie, B.; Stern, C. L.; Goldberg, D. P. *J. Am. Chem. Soc.* **2001**, *123*, 9447−9448.
(21) Ramdhanie, B.; Zakharov, L. N.; Rheingold, A. L.; Goldberg, D. P. *Inorg. Chem.* **2002**, *41*, 4105−4107.
(22) Mandimutsira, B. S.; Ramdhanie, B.; Todd, R. C.; Wang, H. L.; Zareba, A. A.; Czernuszewicz, R. S.; Goldberg, D. P. *J. Am. Chem. Soc.* **2002**, *124*, 15170−15171.
(23) For a recent theoretical study on high-valent corrolazines, see: Tangen, E.; Ghosh, A. *J. Am. Chem. Soc.* **2002**, *124*, 8117−8121.
(24) Liu, H. Y.; Lai, T. S.; Yeung, L. L.; Chang, C. K. *Org. Lett.* **2003**, *5*, 617−620.
(25) Eikey, R. A.; Khan, S. I.; Abu-Omar, M. M. *Angew. Chem., Int. Ed.* **2002**, *41*, 3592−3595.
(26) Vogel, E.; Will, S.; Tilling, A. S.; Neumann, L.; Lex, J.; Bill, E.; Trautwein, A. X.; Wieghardt, K. *Angew. Chem., Int. Ed. Engl.* **1994**, *33*, 731−735.
(27) Van Caemelbecke, E.; Will, S.; Autret, M.; Adamian, V. A.; Lex, J.; Gisselbrecht, J.-P.; Gross, M.; Vogel, E.; Kadish, K. M. *Inorg. Chem.* **1996**, *35*, 184−192.
(28) Simkhovich, L.; Galili, N.; Saltsman, I.; Goldberg, I.; Gross, Z. *Inorg. Chem.* **2000**, *39*, 2704−2705.
(29) Cai, S.; Walker, F. A.; Licoccia, S. *Inorg. Chem.* **2000**, *39*, 3466−3478.
(30) Gross, Z. *J. Biol. Inorg. Chem.* **2001**, *6*, 733−738.
(31) Ghosh, A.; Steene, E. *J. Inorg. Biochem.* **2002**, *91*, 423−436.
(32) Simkhovich, L.; Goldberg, I.; Gross, Z. *Inorg. Chem.* **2002**, *41*, 5433−5439.
(33) Zakharieva, O.; Schunemann, V.; Gerdan, M.; Licoccia, S.; Cai, S.; Walker, F. A.; Trautwein, A. X. *J. Am. Chem. Soc.* **2002**, *124*, 6636−6648.
(34) Will, S.; Lex, J.; Vogel, E.; Adamian, V. A.; Van Caemelbecke, E.; Kadish, K. M. *Inorg. Chem.* **1996**, *35*, 5577−5583.
(35) Jones, R. D.; Summerville, D. A.; Basolo, F. *Chem. Rev.* **1979**, *79*, 139−179.
(36) Smith, T. D.; Pilbrow, J. R. *Coord. Chem. Rev.* **1981**, *39*, 295−383.
(37) A cofacial bis(cobalt) porphyrin−corrole dimer has been reported to bind dioxygen with the cobalt corrole in the +3 oxidation state: Guilard, R.; Jérôme, F.; Gros, C. P.; Barbe, J.-M.; Ou, Z. P.; Shao, J. G.; Kadish, K. M. *C. R. Acad. Sci.* **2001**, *4*, 245−254.

Octa(*tert*-butylphenyl) Cobalt Corrolazine Triphenylsilylacetylide (TBP)$_8$CzCo(CCSiPh$_3$) (2). To a stirring solution of (TBP)$_8$CzCo^{III} (100 mg, 0.071 mmol) in 50 mL of distilled THF was added triphenylsilylacetylene (201 mg, 0.71 mmol). Triethylamine was added (715 mg, 0.71 mmol, 1.0 mL), and the solution was allowed to stir at room temperature for 16 h. The THF and triethylamine were removed under vacuum. The remaining brown residue was then redissolved in a minimal amount of methylene chloride. Purification by silica gel chromatography (neat methylene chloride) afforded a brown solid (70 mg, 58%) R_f = 0.60 (methylene chloride on silica). Free-flowing powdered samples for elemental analysis and SQUID measurements were obtained by precipitation of **2** from toluene/MeOH. ^{1}H NMR (400 MHz, CD_2Cl_2): δ (ppm) 26.4 (br), 21.5 (br), 17.7 (br), 12.5 (br), 10.1 (br), 9.5 (br), 8.6−8.3 (m), 8.1−7.4 (m), 7.2−6.7 (m), 6.8 (m), 6.2 (m), 4.9 (br), 3.6 (br), 2.3 (br), 1.5 (br), −14.0 (br), −20.5 (br). ^{29}Si NMR (79 MHz, CD_2Cl_2): δ (ppm) −28.9. UV−vis (CH_2Cl_2) λ_{max} [nm] ($\epsilon \times 10^{-4}$) 450 (4.0), 619 (1.3), 673 (1.6), 778 (0.8). IR: ν(C≡C) region (KBr) 2062 cm^{-1}. LDI-TOF (negative ion mode): *m*/*z* (% intensity): 1698 (60, M + 1), 1415 (100, M−CCSi(Ph)$_3$). Anal. Calcd for $C_{116}H_{119}N_7Si_1Co\cdot H_2O\cdot 2CH_3OH$: C, 79.61; H, 7.31; N, 5.51. Found: C, 79.21; H, 7.31; N, 6.11.

Formation of [(TBP)$_8$CzCo^{II}(py)]$^-$. UV−Vis Titration. For the reduction of (TBP)$_8$CzCo^{III}(py)$_2$ to [(TBP)$_8$CzCo^{III}(py)]$^-$, it is important to keep the solution scrupulously air-free, and thus a 250-mL Schlenk flask was specially modified to contain a 1-cm path-length quartz cell (total volume ≈ 3 mL) fused to a sidearm assembly which could then be filled by simply tilting the flask and allowing the solution to drain into the sidearm attachment. This setup allowed for the convenient injection of aliquots of reducing agent followed by subsequent stirring of the reaction mixture while minimizing the possibility of exposure to air. The specially modified Schlenk flask was loaded with a stir bar and charged with 10 mL of a green-brown solution of (TBP)$_8$CzCo^{III}(py)$_2$ (9.56×10^{-5} M) in pyridine/EtOH, 1/1 (v/v)). The solution was degassed by sparging with argon, and then 100-μL aliquots of a 0.145 M solution of $NaBH_4$ in ethanol were added in succession, producing a gradual color change from a dark brown-green to a blue-green. After each addition, the reaction mixture was allowed to stir for 5 min to reach equilibrium, and then a UV−vis measurement was taken. The $NaBH_4$ solution was added until no further change was observed in the UV−vis spectrum (total $NaBH_4$ added: 1.1 mL, 0.16 mmol, 166 equiv).

Formation of [(TBP)$_8$CzCo^{II}(py)]$^-$ (3) and [(TBP)$_8$CzCo^{III}(py)(O$_2$)]$^-$ for EPR Spectroscopy. To 100 μL of a solution of (TBP)$_8$CzCo^{III}(py)$_2$ (8.4×10^{-3} M) in pyridine/EtOH (1/1, v/v) was added 100 μL of a solution of $NaBH_4$ (0.145 M) in ethanol in an inert-atmosphere drybox. The solution immediately changed from the brown-green color of (TBP)$_8$CzCo^{III}(py)$_2$ to the blue-green color of [(TBP)$_8$CzCo^{II}(py)]$^-$. The solution was transferred to a quartz EPR tube (4 mm i.d.), sealed with septum/Parafilm, and removed from the glovebox for EPR measurements or further reaction with dioxygen. To generate the cobalt−superoxo complex [(TBP)$_8$CzCo^{III}(py)(O$_2$)]$^-$, an EPR tube containing a freshly prepared solution of [(TBP)$_8$CzCo^{II}(py)]$^-$ was cooled in dry ice (−78 °C) and then bubbled with dry O_2 gas for ∼20 s. There was an immediate color change from blue-green to dark brown, indicating the formation of [(TBP)$_8$CzCo^{III}(py)(O$_2$)]$^-$. The oxygenated solution was then quick-frozen in an N_2(l) bath (−196 °C) and stored at that temperature until it was transferred to the EPR instrument. The spectrum of [(TBP)$_8$CzCo^{II}(py)]$^-$ can be regenerated by thawing the solution to room temperature and bubbling with Ar(g) for ∼10 s. The oxygenation/deoxygenation steps can be cycled ∼3 times, after which the EPR signal for [(TBP)$_8$CzCo^{II}(py)]$^-$ cannot be regenerated unless more sodium borohydride is added to the solution.

Simulations of EPR Spectra. EPR spectra were simulated using the program QPOWA, originally written by R. L. Belford and co-workers[38−40] and subsequently modified by J. Telser. The program uses a standard spin Hamiltonian with matrix diagonalization of a system with $S = {}^1/_2$ coupled to a single nucleus, which is ^{59}Co (100%, $I = {}^7/_2$) in the simulations described here. Additional hyperfine-coupled nuclei are treated using a perturbation theory model. The orientation of the hyperfine coupling matrix can be rotated with respect to the electronic coordinate system (**g** matrix) by Euler angles.[41] For the simulations involving [(TBP)$_8$CzCo^{II}(py)]$^-$, the **g** and **A**(^{59}Co) matrixes were assumed to be collinear, as is standard absent detailed single-crystal EPR studies. However, for the dioxygen-bound complex [(TBP)$_8$CzCo^{III}(py)(O$_2$)]$^-$, such an assumption is not valid because the unpaired spin is predominantly located on the resulting superoxo ligand, and thus the Co complex is effectively a "superhyperfine ligand" to the dioxygenic paramagnet, rather than the normal situation in which a diamagnetic ligand is "superhyperfine" coupled to a paramagnetic metal ion. Single-crystal EPR studies are needed to determine the exact relation between the electronic (**g** matrix) and nuclear (**A**(^{59}Co) matrix) coordinate systems. Such a study has been carried out on the related oxygen adduct of vitamin B_{12} ($B_{12r}O_2$) by Jörin et al.,[42] and thus we used this study as a starting point to obtain a reasonable simulation of the observed frozen solution EPR spectrum for [(TBP)$_8$CzCo^{III}(py)(O$_2$)]$^-$, despite the large parameter space: three ^{59}Co hyperfine matrix components and three Euler angles (even assuming exact knowledge of the **g** matrix). Following Jörin et al., we assume that the largest g value for [(TBP)$_8$CzCo^{III}(py)(O$_2$)]$^-$ (g_3 = 2.075; 2.079 for $B_{12r}O_2$) corresponds to the O−O vector and that the largest A value (A_3 = 60 MHz; 63 MHz for $B_{12r}O_2$) lies in the Cz plane, roughly bisecting the N−Co−N angle. The remaining **g** matrix components also correspond quite closely to those of $B_{12r}O_2$: g_1 = 1.996; 1.994 for $B_{12r}O_2$and g_2 = 2.011; 2.012 for $B_{12r}O_2$. The remaining **A** matrix components are in the range 20−40 MHz and thus are also similar to those determined exactly for $B_{12r}O_2$: A_1 = 21 MHz, A_2 = 27 MHz.

To reproduce the observed EPR spectrum, it is necessary both to "twist" the O−O π-system (defined by g_1 and g_2) with respect to the Cz plane and to "tilt" the O−O σ-bond (defined by $g_3 = g_z$) away from the Cz plane. This is accomplished by rotation about the Euler angles α = 15° and β = 25°, respectively. The uncertainty in these rotation angles is roughly 5°. An additional rotation (by Euler angle γ) would define the projection of the O−O vector in the Cz plane, but our frozen solution data do not warrant this refinement.

SQUID Measurements. The magnetic susceptibility of a powder sample of compounds **1** and **2** were measured between 4 and 300 K with applied magnetic fields of 0.1, 1, and 2 T using a Cryogenic Ltd. S600 SQUID magnetometer. The samples were wrapped in Teflon tape. The data were corrected for the magnetism of the sample holder, which was independently determined at the same temperature range and field. The underlying diamagnetism of the samples was estimated from Pascal's constants.[43] Magnetization measurements were performed on the same sample at 2.5 K with an applied field up to 6 T.

X-ray Crystallography. Crystal data for **2**·(C_7H_8) at 150(2) K: $C_{123}H_{127}CoN_7Si$, M_r = 1790.34, triclinic, $P\bar{1}$, a = 15.7889(11) Å, b = 18.3915(12) Å, c = 19.4754(13) Å, α = 71.026(1)°, β = 73.109(1)°, γ = 89.800(1)°, V = 5091.4(6) Å^3, Z = 2, ρ_{calcd} = 1.168 g cm^{-3}, F(000) = 1910, μ(Mo Kα) = 0.234 mm^{-1}. X-ray diffraction intensities were collected on a Bruker SMART APEX CCD diffractometer (T = 150(2) K, Mo Kα radiation (λ = 0.71073 Å), crystal dimensions: 0.30 × 0.25 × 0.10 mm^{-3}, $2\theta_{max}$ = 56.5°, total number of reflections 31903, independent reflections 22217 [R_{int} = 0.0236]). SADABS[44] absorption correction was applied (T_{min}/T_{max} = 0.858). Structures were solved using direct methods and completed by subsequent difference Fourier

(38) Nilges, M. J. Ph.D. Thesis, University of Illinois, Urbana, IL, 1979.
(39) Belford, R. L.; Nilges, M. J. In *EPR Symposium, 21st Rocky Mountain Conference*; Denver, CO, 1979.
(40) Maurice, A. M. Ph.D. Thesis, University of Illinois, Urbana, IL, 1980.
(41) McGavin, D. G. *J. Magn. Reson.* **1987**, *74*, 19−55.
(42) Jörin, E.; Schweiger, A.; Günthard, H. H. *Chem. Phys. Lett.* **1979**, *61*, 228−232.
(43) Carlin, R. L. *Magnetochemistry*; Springer-Verlag: New York, 1986.
(44) Sheldrick, G. M. *SADABS (2.01)*, Bruker/Siemens Area Detector Absorption Correction Program, Bruker AXS, Madison, Wisconsin, 1998.

Scheme 1

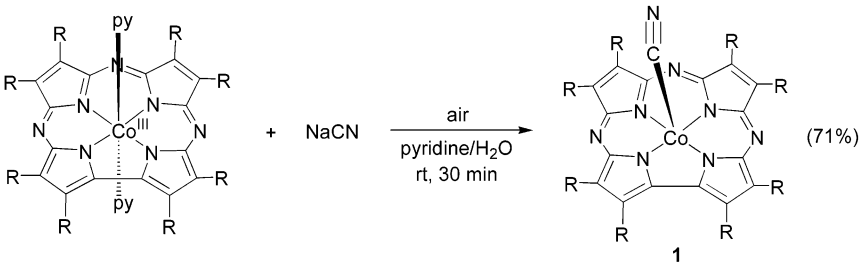

Scheme 2

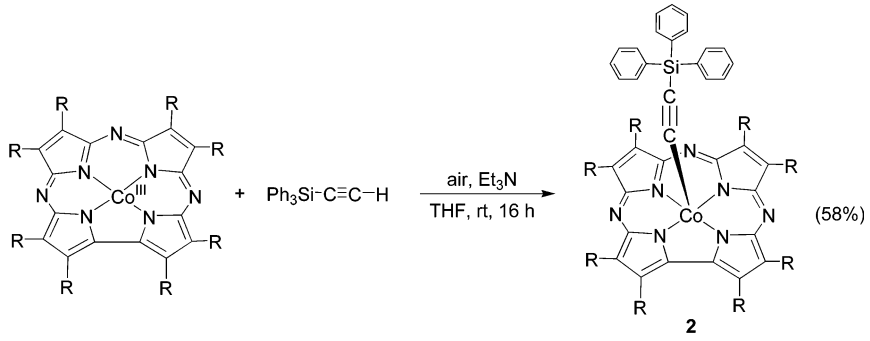

syntheses and refined by full matrix least-squares procedures on F^2. Besides the main molecule **2** in the crystal structure there is a solvate toluene molecule. All non-hydrogen atoms were refined with anisotropic displacement coefficients. The H atoms were placed at calculated positions and refined in a riding group model. Number of refinement parameters is 1187. The final R factors [$I > 2\sigma(I)$]: R1 = 0.1108, wR2 = 0.2650, GoF = 1.126. All software and sources of the scattering factors are contained in the SHELXTL (5.10) program package (G. Sheldrick, Bruker XRD, Madison, WI).

Results and Discussion

Synthesis of (TBP)$_8$CzCo(CN). The synthesis of (TBP)$_8$CzCo(CN) was established according to Scheme 1. Addition of excess sodium cyanide dissolved in water to a pyridine solution of (TBP)$_8$CzCo^{III} in the presence of air leads to an immediate color change (within 1 min) from green to brown. The initial green color is typical for (TBP)$_8$CzCo^{III}(py)$_2$, which is formed in situ at the beginning of the reaction. In the absence of air no color change is noted, even after stirring for 16 h at room temperature. If the anaerobic reaction mixture is then exposed to air, the expected green-to-brown color change takes place. These results point to dioxygen as the necessary oxidant for the formation of the mono-cyano complex and are consistent with **1** being one oxidation level above (TBP)$_8$CzCo^{III}(py)$_2$. The electronic configuration of **1** can be formulated by two extremes: (TBP)$_8$CzCo^{IV}(CN), in which the cobalt is in the +4 oxidation state, or (TBP)$_8$Cz$^{+\bullet}$Co^{III}(CN), in which the "hole" resides on the macrocycle giving a π-cation-radical complex, and it is this latter form that is strongly suggested by its EPR spectrum (vide infra). The crude product was easily purified by standard chromatographic methods (silica gel, eluent methylene chloride) to give **1** in good yield (71%). This complex is stable in both the solid state and in solution at room temperature in the air for several weeks.

The mono-cyano complex can also be prepared by treating the (TBP)$_8$CzCo^{III} starting material with the oxidizing agent (NH$_4$)$_2$Ce^{IV}(NO$_3$)$_6$ followed by reaction with NaCN in water. When ceric ion is used in place of air as the oxidant, a second product is formed which has been identified as the bis-cyano complex, (TBP)$_8$CzCo(CN)$_2$. This complex was initially identified during chromatography as a brown band (silica gel, eluent CH_2Cl_2), which eluted after the mono-cyano product. The bis-cyano complex has been identified by MALDI-MS (M+1, 1467) and IR spectroscopy. The yield for this compound was quite low and difficult to reproduce, and therefore its synthesis was not further pursued, although we were able to confirm the basic connectivity of this complex by X-ray crystallography.[45] Interestingly, there is no evidence for the formation of the bis-cyano complex in the absence of ceric ion. These observations are consistent with the formulation of a higher oxidation level for the bis-cyano species as compared to the mono-cyano complex. The overall oxidation level for **1** is the same as that for the σ-phenyl−corrole complex (OEC)Co(C_6H_5) reported by Vogel and Kadish,[34] which could also be oxidized further by treatment with Fe^{III}(ClO$_4$)$_3$ to give [(OEC)Co(C_6H_5)]$^+$ClO$_4^-$ (OEC = β-octaethylcorrolate). The latter complex was described as a doubly oxidized corrole with a central Co(III) ion.[34,46] Given this precedent, we suggest that the bis-cyano complex is likely doubly oxidized on the ring.

FT-IR Spectroscopy of the Cyano Complex. The FT-IR spectrum of a sample of **1** prepared as a KBr pellet or in solution (CH_2Cl_2) shows two peaks at 2135 and 2198 cm^{-1}, which are clearly different from free C≡N$^-$ (2080 cm^{-1} in aqueous solution) and can be assigned to two different C≡N stretches. It is well-established that the C≡N stretch in general increases upon going from a terminal (M−C≡N) to a bridging (M−C≡N−M) coordination mode in metal−cyanide compounds.[47] The

(45) The X-ray structure of this complex was of low quality because the crystal was weakly diffracting, but the Co(CN)$_2$ structure was confirmed. The quality of the structure, however, was not good enough to provide definitive information regarding the oxidation state.
(46) Harmer, J.; Van Doorslaer, S.; Gromov, I.; Bröring, M.; Jeschke, G.; Schweiger, A. *J. Phys. Chem. B* **2002**, *106*, 2801−2811.
(47) Nakamoto, K. *Infrared and Raman Spectra of Inorganic and Coordination Compounds*, 5th ed.; John Wiley & Sons: New York, 1997.

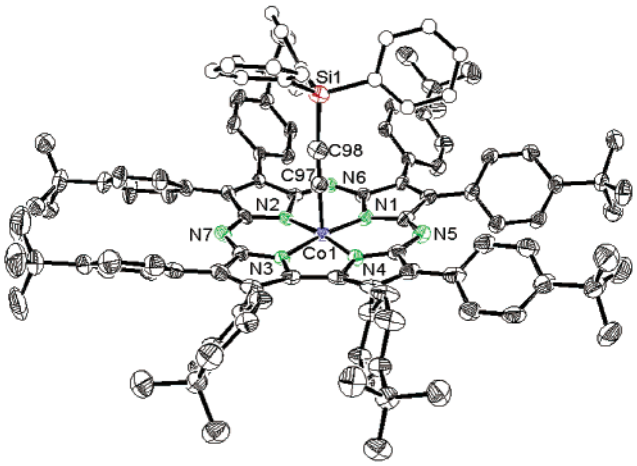

Figure 1. ORTEP diagram of $(TBP)_8CzCo(CCSiPh_3)$ (**2**). Thermal ellipsoids are drawn at a 50% probability level, and hydrogen atoms have been omitted for clarity.

peak at 2135 cm^{-1} is similar to the ν(C≡N) stretch (2130 cm^{-1}) for the monomeric phthalocyanine (Pc) compound $[PcCo^{III}(CN)_2]^-$,[48] which contains terminal cyanide ligands, whereas the peak at 2198 cm^{-1} corresponds to a bridging M−C≡N−M stretch; compare ν(C≡N) = 2158 cm^{-1} for polymeric $[PcCo^{III}(CN)]_n$, in which the cyanide ligand is bridging between cobalt centers.[48] The higher frequency stretch at 2198 cm^{-1} for **1** is also quite close to that reported for $[(OEP)Co(CN)]_n$ (OEP = octaethylporphyrin), which has ν(C≡N) = 2186 cm^{-1} and is described as having a bridged M−C≡N−M polymeric structure.[49] Thus $(TBP)_8CzCo(CN)$ likely exists in both monomeric and cyanide-bridged forms. Interestingly, the IR spectrum for the bis-cyano complex $(TBP)_8CzCo(CN)_2$ in KBr exhibits only one peak at 2189 cm^{-1}. This stretching frequency may indicate bridging cyanides, although the 2:1 (CN:Co) formula would be more consistent with terminal cyanide ligands. Other factors, such as oxidation state and electronegativity of the metal center, can also affect the stretching frequency. In general, an increase in oxidation state or electronegativity causes stronger σ-donation from CN^-, which results in a higher frequency because electrons are being removed from an antibonding (with respect to the C−N bond) orbital.[47] Thus, the high C≡N stretch for the bis-cyano complex may be reflective of the higher oxidation state for Co in this complex, rather than a bridging mode for CN^-.[50]

^{1}H NMR, EPR, and Magnetic Susceptibility of $(TBP)_8CzCo(CN)$. The ^{1}H NMR spectrum of **1** shows broad resonances in the aromatic region corresponding to the peripheral phenyl substituents, and a broad singlet between 1.4 and 1.20 ppm arising from the *tert*-butyl groups. The broadness of the peaks is likely due to the presence of the paramagnetic, monomeric form. Further information concerning the electronic configuration was obtained by EPR spectroscopy.

The EPR spectrum at 298 K for the mono-cyano complex dissolved in toluene reveals a singlet centered at $g = 2.0021$ with a peak-to-trough separation of 12 G. A similar spectrum is obtained at low temperature in frozen solution (25 K), with $g = 2.0038$ and 26 G peak-to-trough separation. This signal is indicative of a π-cation-radical-type compound, since there is no observable hyperfine coupling from the cobalt ion and no significant g anisotropy at low temperature. However, the line width at low temperature is slightly larger than a typical porphyrin[51,52] or phthalocyanine[53,54] π-cation-radical and may indicate a small amount of delocalization on to the cobalt center. The magnetic susceptibility of **1** was measured between 4 and 300 K by a SQUID magnetometer and revealed diamagnetic behavior throughout the temperature range. This behavior is consistent with the presence of strong antiferromagnetic (AF) coupling between molecules. Although the structure of this material has not been characterized by X-ray crystallography, the solid-state IR data discussed above show the presence of cyanide bridges, which are expected to provide a pathway for strong antiferromagnetic coupling. In addition, porphyrin π-cation-radicals are well known to aggregate in both the solution- and solid state through π-stacking interactions and as a consequence to exhibit direct spin-pairing via $\pi-\pi$ overlap.[55] This kind of direct spin-pairing mechanism may also be responsible for the quenching of the magnetic moment.

Synthesis of $(TBP)_8CzCo(CCSiPh_3)$. We were unable to grow X-ray quality crystals of the mono-cyano complex. In our previous experience we have had much better success in growing X-ray quality crystals of $(TBP)_8CzML_n$ complexes that contain large axial ligands, and thus we decided to prepare the triphenylsilylacetylide complex **2**, with the knowledge that a terminal alkynyl ligand is isoelectronic with CN^-. The synthesis of **2** is shown in Scheme 2. The cobalt complex $(TBP)_8CzCo^{III}$ was combined with 10 equiv of triphenylsilylacetylene and triethylamine in THF under aerobic conditions. The reaction mixture was stirred for 16 h at room temperature to give crude $(TBP)_8CzCo(CCSiPh_3)$, which was purified by chromatography (silica gel, methylene chloride) to afford the cobalt acetylide complex in good yield (58%). This complex was then crystallized from toluene/MeOH to give crystals of X-ray quality. If air is excluded from the reaction mixture, no product is formed after stirring for 16 h at room temperature. The presence of air is essential for the reaction to proceed, indicating O_2 is the active oxidant, as found for the mono-cyano complex.

Structure and Bonding in the Acetylide Complex. An ORTEP diagram of $(TBP)_8CzCo(CCSiPh_3)$ is shown in Figure 1, and selected bond distances and angles are presented in Table 1 together with those for $(TBP)_8CzCo^{III}(PPh_3)$ and $(TBP)_8CzCo^{III}(py)_2$ for comparison. The macrocycle is relatively planar, with the largest deviation from the average plane of the 23 core atoms being 0.187(3) Å and the mean deviation being 0.107 Å. The cobalt ion sits almost directly in the plane (d(Co-plane) = −0.076(1) Å) and is 0.092(2) Å above the plane formed by the four pyrrole nitrogen atoms, in contrast to the other five-coordinate complex $(TBP)_8CzCo^{III}(PPh_3)$, which shows the cobalt ion sitting significantly out of the plane toward the axial ligand. Interestingly, there is an umbrella shape to **2**, with the acetylide forming the "handle" and the macrocycle domed slightly toward the $-CCSiPh_3$ unit.

(48) Hanack, M. *Mol. Cryst. Liq. Cryst.* **1984**, *105*, 133−149.
(49) Fahmy, N.; Leverenz, A.; Hanack, M. *Synth. Met.* **1991**, *41*−*43*, 2615−2619.
(50) Geiss, A.; Vahrenkamp, H. *Inorg. Chem.* **2000**, *39*, 4029−4036.
(51) Fajer, J.; Borg, D. C.; Forman, A.; Dolphin, D.; Felton, R. H. *J. Am. Chem. Soc.* **1970**, *92*, 3451−3459.
(52) Kalsbeck, W. A.; Seth, J.; Bocian, D. F. *Inorg. Chem.* **1996**, *35*, 7935−7937.
(53) Myers, J. F.; Canham, G. W. R.; Lever, A. B. P. *Inorg. Chem.* **1975**, *14*, 461−468.
(54) Ough, E.; Gasyna, Z.; Stillman, M. J. *Inorg. Chem.* **1991**, *30*, 2301−2310.
(55) Fuhrhop, J. H.; Wasser, P.; Riesner, D.; Mauzerall, D. *J. Am. Chem. Soc.* **1972**, *94*, 7996.

Table 1. Selected Bond Lengths (Å) and Bond Angles (deg) for $(TBP)_8CzCo(CCSiPh_3)$, $(TBP)_8CzCo^{III}(PPh_3)$, and $(TBP)_8CzCo^{III}(py)_2$

	$(TBP)_8CzCo(CCSiPh_3)$	$(TBP)_8CzCo^{III}(PPh_3)$[a]	$(TBP)_8CzCo^{III}(py)_2$[a]
Co−N(1)	1.834(3)	1.838(3)	1.838(3)
Co−N(2)	1.827(3)	1.852(3)	1.850(4)
Co−N(3)	1.815(3)	1.826(3)	1.830(3)
Co−N(4)	1.812(3)	1.834(3)	1.834(3)
Co−L[b]	1.831(4)	2.1747(12)	2.000(4), 1.970(4)
$Co-(N(1)-N(4))_{plane}$	0.092(2)	0.288	0.006
$Co-(23\text{-atom})_{core}$	−0.076(1)	0.442	0.084
$C_\beta-C_\beta$ (av)	1.373(12)	1.381(11)	1.390(12)
$C_\alpha-C_\beta$ (av)	1.456(12)	1.446(16)	1.448(17)
$C_\alpha-C_\alpha$	1.502(6)	1.492(6)	1.459(6)
N(1)···N(3)	3.640(5)	3.638	3.678
N(2)···N(4)	3.691(5)	3.612	3.663
C(97)≡C(98)	1.194(7)		
N(1)−Co−N(2)	93.84(15)	92.29(13)	94.51(15)
N(2)−Co−N(3)	91.49(14)	89.44(14)	91.39(15)
N(3)−Co−N(4)	82.97(14)	82.10(14)	83.06(13)
N(4)−Co−N(1)	91.13(14)	90.53(14)	91.06(15)
N(1)−Co−L[a]	94.51(18)	105.49(10)	89.83(16), 86.60(16)
N(2)−Co−L[a]	94.70(17)	99.31(10)	89.34(16), 91.05(16)
N(3)−Co−L[a]	91.06(17)	92.89(10)	91.58(16), 91.95(16)
N(4)−Co−L[a]	91.56(17)	97.56(10)	90.07(15), 89.88(16)

[a] See ref 21. [b] L = axial ligand.

The Co−N(av) distance of 1.82(1) Å for **2** is slightly smaller than the Co−N(av) distance of 1.838(9) Å found for both $(TBP)_8CzCo^{III}(PPh_3)$ and $(TBP)_8CzCo^{III}(py)_2$. This may be a reflection of the higher oxidation level of the cobalt center in the acetylide complex. Interestingly, the Co−C bond length in **2**, 1.831(4) Å, is among the shortest known for any M−C≡CR complex.[56,57] A search of the Cambridge Structural Database[58] shows that there are no other Co−C≡CR porphyrinoid complexes for direct comparison, and thus one of the closest analogues is the Co(III) complex Co(DO)(DOH)pn(C≡CSiMe$_3$)(I) ($(DO)(DOH)_{pn}$ = 1,3-bis(diacetylmonoximeimino)propane), which has a planar array of N_4 donor atoms from an oxime-based ligand and a trimethylsilylacetylide axial ligand.[59] The Co−C distance of 1.948(5) Å for this complex is significantly longer than that found for **2**, although it should be pointed out that in the former complex there is an iodide ligand coordinated trans to the acetylide group. The only other known corrole Co−C bond distances come from (OEC)Co(Ph) and $[(OEC)Co(Ph)]^+ClO_4^-$, which have Co−C distances of 1.937(3) and 1.970(7) Å, respectively.[34] The short Co−C distance in **2** can be attributed to either π-back-bonding or to a strong σ-type interaction resulting from a high oxidation state cobalt ion.[57] If M−CCR π-interactions were significant, a lengthening of the −C≡CR bond would be expected; however, this distance in **2** (1.194(7) Å) is close to the mean value (1.201(16) Å) of known MC≡CR bond lengths.[57,60] In addition, the stretching frequency ν(C≡C) would be expected to weaken in the presence of M−CCR π-back-bonding. By comparing ν(C≡C) for **2** (2062 cm^{-1}) with that of triphenylsilylacetylene (2036 cm^{-1})[61] or Co(DO)(DOH)pn(C≡CSiMe$_3$)(I) (2040 cm^{-1}), it is clear that there is a small *strengthening* in ν(C≡C) for **2**. A slight increase in ν(C≡C) for **2** correlates with a strong σ-type interaction for the M−C bond.[56] Taken together, the structural and vibrational data are in favor of a strong M−C σ-interaction due to a high oxidation state cobalt ion.

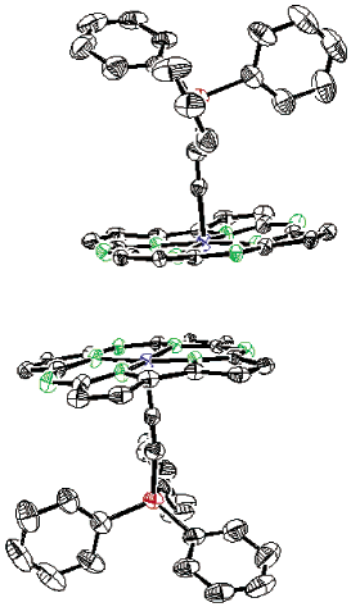

Figure 2. Fragment of the crystal structure of **2**·(C_7H_8) showing the π-stacking interaction. Solvent molecule and all hydrogen atoms and peripheral 4-*tert*-butylphenyl substituents in **2** have been omitted for clarity.

As shown in the packing diagram of Figure 2, the acetylide complex forms a π-stacked dimer pair in the solid state. The π-stacking interaction is characterized by the geometric parameters given in Table 2, which have been developed previously for the classification of porphyrin $\pi-\pi$ dimers.[62] In general, the π-interactions are sensitive to the level of ring oxidation, and the mean-plane-separation (mps), lateral shift (l.s.) and slip angle (θ) follow the trend: π-cation-radical < neutral porphyrin; an oxidized ring system typically has a tighter $\pi-\pi$ interaction and much greater cofacial overlap. For the few corrole examples

(56) Nast, R. *Coord. Chem. Rev.* **1982**, *47*, 89−124.
(57) Manna, J.; John, K. D.; Hopkins, M. D. *Adv. Organomet. Chem.* **1995**, *38*, 79−154.
(58) Allen, F. H. *Acta Crystallogr., Sect. B* **2002**, *58*, 380−388.
(59) Giese, B.; Zehnder, M.; Neuburger, M.; Trach, F. *J. Organomet. Chem.* **1991**, *412*, 415−423.
(60) Vaid, T. P.; Veige, A. S.; Lobkovsky, E. B.; Glassey, W. V.; Wolczanski, P. T.; Liable-Sands, L. M.; Rheingold, A. L.; Cundari, T. R. *J. Am. Chem. Soc.* **1998**, *120*, 10067−10079.
(61) Naka, A.; Ishikawa, M. *J. Organomet. Chem.* **2000**, *611*, 248−255.
(62) Scheidt, W. R.; Brancato-Buentello, K. E.; Song, H.; Reddy, K. V.; Cheng, B. *Inorg. Chem.* **1996**, *35*, 7500−7507.

Table 2. Comparison of Geometric Parameters for $\pi-\pi$ Dimers in Porphyrins, Corroles, and **2**[a]

	2	Porph$^{+\bullet}$[62,b]	Porph[62,b]	(OEC)Co(Ph)[34]	[(OEC)Co(Ph)]$^+$[34]	(OEC)Fe(NO)]$^+$[63]
M−M	4.351	−	−	5.33	4.13	3.96
Ct−Ct[c]	4.457	3.26(6)	4.94(24)	−	−	−
mps[d]	3.47	3.25(6)	3.55(14)	3.50	3.45	3.21
l.s.[e]	2.712	0.1(6)	3.48(47)	3.67[f]	1.66[f]	−
slip angle (θ)	37.5	1.74(1.11)	43.8(3.6)	46.0[f]	25.39[f]	−

[a] Distances in Å, angles in deg. [b] Porph = neutral porphyrin. [c] Ct = centroid of the porphyrinoid core. [d] mps = mean-plane-separation. [e] l.s. = lateral shift. [f] Calculated from data obtained from the Cambridge Structural Database (see ref 58).

Table 3. EPR Parameters for $[(TBP)_8CzCo^{II}(py)]^-$ and Co^{II}−Corrin, − Porphyrin, −Phthalocyanine, and −Corrole Complexes[a]

	g_x	g_y	g_z	$A_x^{Co,b}$	$A_y^{Co,b}$	$A_z^{Co,b}$	$A_z^{N,b}$	ref
$[(TBP)_8CzCo^{II}(py)]^-$	2.40	2.20	1.98	40	40	340	60[c]	this work
B_{12r}[d]	2.310	2.190	2.004	65 ± 12	80 ± 12	302 ± 10	53 ± 2	80
(TCTDH)Co(py)	2.44	2.16	2.001	114[e]	56[e]	277[e]	42[e]	75
$(OEP)Co^{II}(py)$	$g_\perp = 2.26$; $g_\parallel = 2.025$			$A_\perp \le 25$; $A_\parallel = 231$			$A_\parallel = 44$	70
$(Pc)Co^{II}$(4-Mepy)	$g_\perp = 2.32$; $g_\parallel = 2.005$			$A_\perp = 42$[e]; $A_\parallel = 274$[e]			$A_\parallel = 45$[e]	74
$[(DHC)Co^{II}]^-$	2.776	2.321	1.966	392[e]	286[e]	132[e]	−	84
$[(OMTPC)Co^{II}]^-$	3.349	2.187	1.903	507[e,f]	213[e,f]	−	−	85
$[(MEC)Co^{II}]^-$[,g]	3.236	2.263	1.847	507[e,f]	291[e,f]	−	−	87
$[(PMC)Co^{II}]^-$[,g]	3.242	2.214	1.848	507[e,f]	302[e,f]	−	−	87
$[(MEC)Co^{II}(py)]^-$[,g]	3.223	2.206	1.848	504[e,f]	316[e,f]	−	48[e,h]	87
$[(PMC)Co^{II}(py)]^-$[,g]	3.225	2.147	1.854	482[e,f]	274[e,f]	−	49[e,h]	87

[a] Abbreviations: B_{12r} = five-coordinate cob(II)alamin; TCTDH = 5,7,12,14-tetramethyldibenzo[*b*,*i*][1,4,8,11]tetraazacyclotetradecahexaene; DHC = 8,12-diethyl-2,3,7,13,17,18-hexamethyl corrole; OMTPC = 5,10,15-triphenyl-2,3,7,8,12,13,17,18-octamethylcorrole; MEC = 2,3,17,18-tetramethyl-7,8,12,13-tetraethylcorrole; PMC = 8,12-bis[2-(ethoxycarbonyl)ethyl]-2,3,7,13,17,18-hexamethylcorrole. [b] *A* values in MHz. [c] $A_x^N = A_y^N = 10$ MHz. [d] Combined X-band/Q-band data on a single-crystal of B_{12r} doped in B_{12b}. B_{12b} = hydroxocob(III)alamin. [e] Converted from cm^{-1} units using 1×10^{-4} $cm^{-1} = 2.8$ MHz. [f] *A* values given as A_1^{Co}, A_2^{Co}, and A_3^{Co}. [g] *g* values given as g_1, g_2, and g_3. [h] Listed as A_2^N.

available, a similar trend seems to hold: the π-stacking interaction in (OEC)Co(Ph) is weaker than that for (OEC)Co(Ph)$^+$ as shown by the slightly smaller M−M distance and considerably smaller lateral shift for the latter complex. A similar tight stacking interaction is seen for the Fe(III) π-cation-radical complex $[(OEC)Fe(NO)]^+$.[63] From this standpoint it is clear that the structural parameters for **2** are more aligned with the properties of a neutral ring system than that of an oxidized π-cation-radical.

Magnetic Susceptibility and EPR Spectroscopy for $(TBP)_8CzCo(CCSiPh_3)$. The magnetic susceptibility of a powder sample of **2** was measured in the range 4−300 K by a SQUID magnetometer. As found for the cyanide complex, the data reveal diamagnetic behavior for **2**, which can be attributed to spin−spin coupling mediated by π-stacking interactions. Definitive structural evidence for the presence of such π-stacking was lacking for the cyanide complex, but the X-ray structure of **2** provides concrete proof that close $\pi-\pi$ overlap is favored for this complex (Figure 2). Interestingly, the closely related corrole complex (OEC)Co(Ph) exhibits a similarly strong intermolecular spin−spin interaction which is mediated by a π-stacking interaction (Table 2) and gives rise to a singlet ground state.[34]

The EPR spectrum of **2** in toluene at 56 K is shown in Figure 3. This spectrum is dramatically different from the simple π-cation-radical-type spectrum seen for the isoelectronic monocyano complex. The spectrum for **2** has a full width of ~150 G, and the central line is located at $g = 2.0$. There appears to be hyperfine splitting on both the low-field and high-field sides of the spectrum, with the features to the high-field side more clearly resolved. At first glance these features appear to be hyperfine splitting from the cobalt nucleus. Initial attempts to

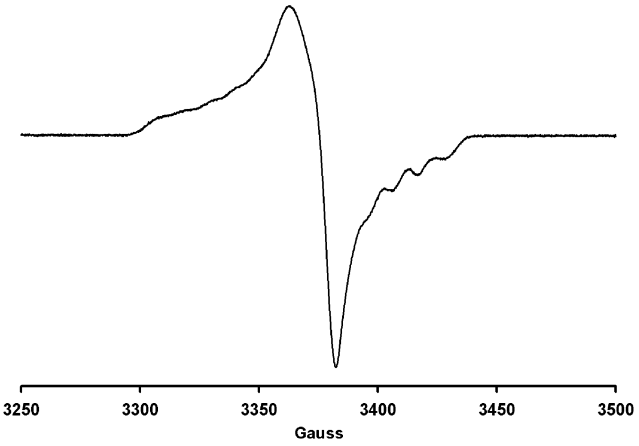

Figure 3. EPR spectrum of $(TBP)_8CzCo(CCSiPh_3)$ in toluene at 56 K. Conditions: frequency, 9.478 GHz; incident microwave power, 4.72 mW; modulation frequency, 100 kHz; modulation amplitude 1.0 G; receiver gain, 8.93×10^4.

simulate this spectrum as a cobalt(IV) complex (i.e., $(TBP)_8CzCo^{IV}(CCSiPh_3)$) by using a combination of *g* anisotropy and ^{59}Co hyperfine coupling did not give satisfactory results. We then attempted to simulate the spectrum by assuming the electronic configuration was best described as a π-cation-radical, $(Cz^{+\bullet})Co^{III}(CCSiPh)_3$, with the observed fine structure due to splitting from the four equivalent ^{14}N nuclei of the pyrrole rings; such splitting from equivalent N-pyrrole atoms has been seen for certain porphyrin π-cation-radicals (e.g. $Zn(TPP^{+\bullet})$).[51,64] These simulations also did not fully reproduce the experimental spectrum, nor did simulations in which different combinations of ^{14}N and ^{59}Co hyperfine interactions were included.[65]

From the EPR data and structural analysis of **2** we conclude that this complex is clearly not well represented as a pure

(63) Autret, M.; Will, S.; Van Caemelbecke, E.; Lex, J.; Gisselbrecht, J.-P.; Gross, M.; Vogel, E.; Kadish, K. M. *J. Am. Chem. Soc.* **1994**, *116*, 9141−9149.

(64) Fajer, J.; Davis, M. S. In *The Porphyrins*; Dolphin, D., Ed.; Academy Press: New York, 1979; Vol. IV, p 197.

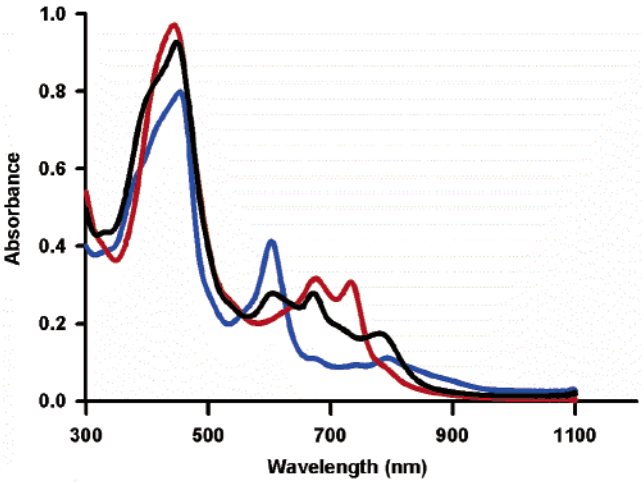

Figure 4. UV−vis spectra of 1.38×10^{-4} M $(TBP)_8CzCo^{III}$ (blue), 2.11×10^{-5} M, $(TBP)_8CzCoCN$ (red), and 2.29×10^{-5} M $(TBP)_8CzCo(CCSiPh_3)$ (black) in CH_2Cl_2.

cobalt(IV) complex, nor is it fully described by a pure π-cation-radical configuration. A similar conclusion was reached by Kadish, Vogel, and co-workers for the analogous corrole complex (OEC)Co(Ph), for which EPR and other spectroscopic measurements point toward the best description of the electronic configuration as the resonance hybrid $(OEC)Co^{IV}(Ph) \leftrightarrow (OEC^{+\bullet})Co^{III}(Ph)$.[34] A recent study of the same complex involving detailed pulsed EPR/ENDOR measurements and DFT calculations by Schweiger and co-workers yields a description of the electronic configuration with 65% spin density residing on the macrocycle and 35% spin density located in a cobalt d_{yz} orbital.[46] We believe an analogous situation holds for **2**, in which the electronic configuration is best represented by the resonance hybrid $(Cz)Co^{IV}(CCSiPh)_3 \leftrightarrow (Cz^{+\bullet})Co^{III}(CCSiPh)_3$, although the spin distribution may be quite different from that calculated for (OEC)Co(Ph).

UV−Vis Spectra of $(TBP)_8CzCo(CCSiPh_3)$, $(TBP)_8CzCo(CN)$, and $(TBP)_8CzCo^{III}$. The UV−vis spectra of the three cobalt complexes $(TBP)_8CzCo$, **1** and **2** are shown in Figure 4. All three complexes exhibit an intense Soret band near 445 nm, but there are distinct differences in the Q-band region (600−900 nm). For the mono-cyano and acetylide complexes there is an obvious red-shift in the Q-band region as compared to the $(TBP)_8CzCo^{III}$ starting material. A similar effect was noted for $(TBP)_8CzCo^{III}(PPh_3)$ and $(TBP)_8CzCo^{III}(py)_2$; the binding of axial PPh_3 or pyridine ligands to $(TBP)_8CzCo^{III}$ caused a red-shift in the Q-band from 600 to 670 nm.[21] For **1** and **2** the spectra are complicated by the fact that these complexes not only contain strong axial ligands, but are also oxidized by one electron. Interestingly, **1** and **2** show rather different UV−vis spectra even though they are isoelectronic. The discrepancies between the spectra for these compounds are likely more of a reflection of the electronic configuration (π-cation-radical for **1** vs the resonance hybrid description for **2**) than a reflection of the identity of the axial ligands.

Formation of $[(TBP)_8CzCo^{II}(py)]^-$ (3). UV−vis Studies. The addition of excess $NaBH_4$(aq) to $(TBP)_8CzCo^{III}$ in a mixture of pyridine/EtOH (50/50 v/v) resulted in the generation of the reduced complex $[(TBP)_8CzCo^{II}(py)]^-$, as shown in Scheme 3. This reaction was monitored by UV−vis spectroscopy, and the data are shown in Figure 5. The initial spectrum prior to the addition of any $NaBH_4$ corresponds to that previously reported for $(TBP)_8CzCo^{III}(py)_2$, with λ_{max} 445, 670 nm.[21] As successive amounts of $NaBH_4$ are added, there is a dramatic change in the UV−vis spectrum. The Q-band at 670 nm rapidly decreases, and two new peaks at 615 and 769 nm appear. In addition, the Soret band at 445 nm increases slightly along with a shoulder at 472 nm. There is tight isosbestic behavior throughout the reduction, and no evidence for other intermediates or products other than the reduced $[(TBP)_8CzCo^{II}(py)]^-$. A large excess of $NaBH_4$ (166 equiv) is needed to drive the reaction to completion. Further additions of $NaBH_4$ had no effect on the spectrum. The final spectrum is stable for many hours, as long as air is strictly excluded. If the solution is exposed to air, the spectrum immediately reverts back to the original spectrum of the cobalt(III) bis-pyridine complex. The data clearly demonstrate that the UV−vis spectrum is quite sensitive to a change in cobalt oxidation state, and show that the cobalt(III) complex is cleanly and quantitatively reduced by $NaBH_4$ to the cobalt(II) product.

$[(TBP)_8CzCo^{II}(py)]^-$. EPR Spectroscopy. The reduced complex $[(TBP)_8CzCo^{II}(py)]^-$ was characterized by EPR spectroscopy, as shown in Figure 6. There is a wealth of information available on the characteristic EPR spectra of cobalt(II) porphyrins,[35,36,66−71] phthalocyanines,[72−74] and other tetradentate ligands (e.g., Schiff's base systems),[35,75,76] and the spectrum in Figure 6 is similar to the spectra in many of these earlier studies. In general, the EPR spectrum of **3** is typical of a five-coordinate, low-spin d^7 Co(II) complex, in which the unpaired electron lies in an orbital predominantly d_{z^2} in character (vide infra). The spectrum exhibits rhombic symmetry, and there is a clear splitting in the high-field region due to hyperfine coupling between the unpaired electron and the ^{59}Co nucleus ($I = {}^7/_2$). There are six broad peaks visible for the expected eight-line splitting pattern from the cobalt nucleus, with the remaining two components obscured by overlap with the features to lower field. A hyperfine coupling of $A_z^{Co} = 340$ MHz is easily obtained by inspection of the spectrum. In addition, a more closely spaced three-line splitting pattern is seen for some of the peaks on the high-field side. Such a pattern is typical for a hyperfine interaction with a *single* nitrogen atom (^{14}N, $I = 1$, $A_z^N = 60$ MHz), indicating that the cobalt(II) corrolazine species has one coordinated pyridine ligand in an axial position. The cobalt and nitrogen hyperfine interactions are similar to the other five-coordinate complexes listed in Table 3.

The best simulation of this spectrum (red line) is also given in Figure 6, and the g and A values used for the simulated

(65) An insightful reviewer suggested that an alternative configuration may arise from a ground state that involves spin density which is localized on the three *meso* nitrogen atoms. Indeed, simulations involving $3 \times {}^{14}N$ nuclei were quite similar to $4 \times {}^{14}N$ simulations but were not much of an improvement on the whole.

(66) Walker, F. A. *J. Magn. Reson.* **1974**, *15*, 201−218.
(67) Walker, F. A. *J. Am. Chem. Soc.* **1970**, *92*, 4235−4244.
(68) Basolo, F.; Hoffman, B. M.; Ibers, J. A. *Acc. Chem. Res.* **1975**, *8*, 384−392.
(69) Van Doorslaer, S.; Schweiger, A. *Phys. Chem. Chem. Phys.* **2001**, *3*, 159−166.
(70) Baumgarten, M.; Winscom, C. J.; Lubitz, W. *Appl. Magn. Reson.* **2001**, *20*, 35−70.
(71) Ozarowski, A.; Lee, H. M.; Balch, A. L. *J. Am. Chem. Soc.* **2003**, *125*, 12606−12614.
(72) Assour, J. M. *J. Am. Chem. Soc.* **1965**, *87*, 4701−4706.
(73) Assour, J. M.; Kahn, W. K. *J. Am. Chem. Soc.* **1965**, *87*, 207.
(74) Cariati, F.; Galizzioli, D.; Morazzoni, F.; Busetto, C. *J. Chem. Soc., Dalton Trans.* **1975**, 556−561.
(75) Pezeshk, A.; Greenaway, F. T.; Dabrowiak, J. C.; Vincow, G. *Inorg. Chem.* **1978**, *17*, 1717−1725.
(76) Pezeshk, A. *Inorg. Chem.* **1992**, *31*, 2282−2284.

Scheme 3

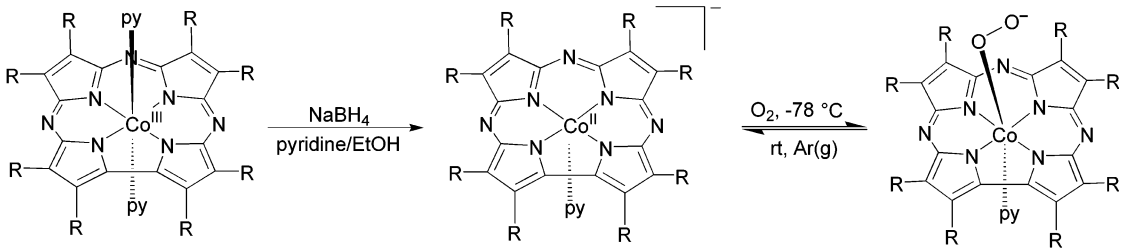

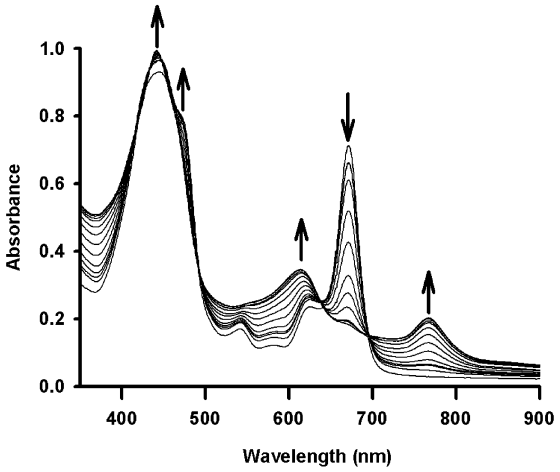

Figure 5. UV−vis titration for the reduction of $(TBP)_8CzCo^{III}(py)_2$ (9.56×10^{-5} M in pyridine) with $NaBH_4$ (0.145 M in EtOH) to give $[(TBP)_8CzCo^{II}(py)]^-$ under argon at room temperature.

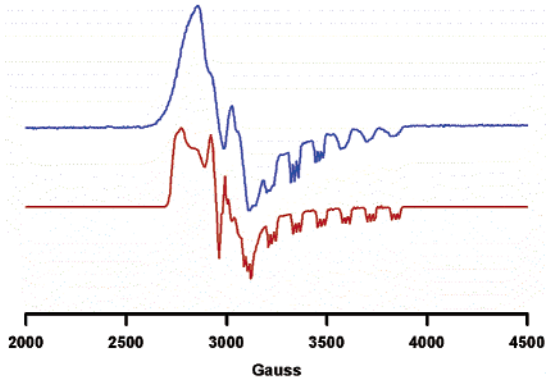

Figure 6. Experimental (blue) and simulated (red) EPR spectrum of $[(TBP)_8CzCo^{II}(py)]^-$ in pyridine/EtOH (50/50 v/v) at 77 K. Experimental conditions: frequency, 9.304 GHz; incident microwave power, 12.69 mW; modulation frequency, 100 kHz; modulation amplitude, 1.0 G; receiver gain, 1.59×10^4. Simulation parameters: $\mathbf{g} = [1.985, 2.200, 2.400]$, $\mathbf{A}(^{59}Co) = [40.0, 40.0, 340.0]$ MHz, $\mathbf{A}(^{14}N) = [10.0, 10.0, 60.0]$ MHz, single-crystal Gaussian line width (hwhm) matrix, $\mathbf{W} = [60, 60, 30]$ MHz.

spectrum are listed in Table 3 together with the parameters for other analogous Co(II) complexes. The majority of Co^{II} porphyrins and phthalocyanines, such as $(OEP)Co^{II}(py)$[70] and $(Pc)Co^{II}(4\text{-Mepy})$[74] listed in Table 3, exhibit an EPR spectrum with axial symmetry. In contrast, a rhombic spectrum is seen for the corrolazine complex, which can be explained by the lower in-plane symmetry of the contracted corrolazine nucleus. The cobalt(II) corrin from vitamin B_{12}[77−80] is more appropriate for comparison in this regard because of its contracted ring structure.

Indeed, under the right conditions, similar rhombic EPR parameters have been observed for vitamin B_{12} (B_{12r} in Table 3).[80] Along the same lines, many Schiff's base complexes, which also have reduced in-plane symmetry, exhibit rhombic EPR spectra.[35,75,76] For example, the TCTDH complex in Table 3 has been studied in detail by EPR spectroscopy and exhibits *g* and *A* values quite similar to those of the corrolazine complex. The rhombic splitting for this complex was attributed to the alternating five- and six-membered chelate rings of the Schiff's base ligand.[75]

Theoretical treatments for the spin Hamiltonian parameters of low-spin (d^7) cobalt(II) complexes have been developed by several workers,[81−83] in which the *g* and *A* values can be related to the ground-state electronic configuration and the energy separations of low-lying doublet and quartet excited states. We have not attempted to apply these equations here, but are nonetheless able to benefit from the previous application of these equations to come to the conclusion that the ground state for **3** is best described as d_{z^2} based on the observed *g* and *A* values for this complex. For example, the *g* and *A* parameters for the TCTDH complex (Table 3) are similar to those for the corrolazine complex, and a detailed theoretical treatment by the authors in this case led to the conclusion that the ground state is clearly d_{z^2} ($(d_{x^2-y^2}d_{xz}d_{yz})^6d_{z^2}{}^1$).[75]

Interestingly, the few examples of Co^{II}−corroles that have been reported exhibit dramatically different EPR spectra as compared to the other complexes in Table 3, in part because they have a marked tendency to remain four-coordinate and not bind axial ligands. The previous $[(corrole)Co^{II}]^-$ anionic complexes were generated by chemical reduction in a fashion similar to **3**. Hush and Woolsey described the generation of $[(DHC)Co^{II}]^-$ (no axial ligands) by reduction of $(DHC)Co^{III}$ with sodium film in THF; however, attempts to form a five-coordinate pyridine adduct were unsuccessful.[84] Boschi and Kadish produced $[(OMTPC)Co^{II}]^-$ via bulk electroreduction of $(OMTPC)Co^{III}(PPh_3)$, finding that the PPh_3 axial ligand apparently dissociates after reduction to generate a four-coordinate species.[85] Only Murakami and co-workers have observed the binding of axial ligands to cobalt(II) corroles.[86,87] The EPR signals for both four-coordinate $[(MEC)Co^{II}]^-$ and $[(PMC)Co^{II}]^-$ (obtained by reduction with $NaBH_4$) and five-coordinate $[(MEC)Co^{II}(py)]^-$ and $[(PMC)Co^{II}(py)]^-$ complexes (^{14}N hy-

(77) Schrauzer, G. N.; Lee, L.-P. *J. Am. Chem. Soc.* **1968**, *90*, 6541−6543.
(78) Schrauzer, G. N.; Lee, L.-P. *J. Am. Chem. Soc.* **1970**, *92*, 1551−1556.
(79) Hamilton, J. A.; Yamada, R.; Blakley, R. L.; Hogenkamp, H. P. C.; Looney, F. D.; Winfield, M. E. *Biochemistry* **1971**, *10*, 347−355.
(80) Jörin, E.; Schweiger, A.; Günthard, H. H. *J. Am. Chem. Soc.* **1983**, *105*, 4277−4286.
(81) Lin, W. C. *Inorg. Chem.* **1976**, *15*, 1114−1118.
(82) Lin, W. C.; Lau, P. W. *J. Am. Chem. Soc.* **1976**, *98*, 1447−1450.
(83) McGarvey, B. R. *Can. J. Chem.* **1975**, *53*, 2498−2511.
(84) Hush, N. S.; Woolsey, I. S. *J. Chem. Soc., Dalton Trans.* **1974**, 24−34.
(85) Adamian, V. A.; D'Souza, F.; Licoccia, S.; Di Vona, M. L.; Tassoni, E.; Paolesse, R.; Boschi, T.; Kadish, K. M. *Inorg. Chem.* **1995**, *34*, 532−540.
(86) Murakami, Y.; Yamada, S.; Matsuda, Y.; Sakata, K. *Bull. Chem. Soc. Jpn.* **1978**, *51*, 123−129.
(87) Murakami, Y.; Matsuda, Y.; Sakata, K.; Yamada, S.; Tanaka, Y.; Aoyama, Y. *Bull. Chem. Soc. Jpn.* **1981**, *54*, 163−169.

perfine splittings were observed) were recorded.[86,87] For all of the corrole complexes in Table 3, a rhombic spectrum with an unusually high maximum g value (g_1) is observed. The corrole g values have some similarity with the g values reported for a series of (TPP)Co^{II} complexes in the absence of axial bases (e.g. $g_{||} = 3.322$, $g_{\perp} = 1.798$ for (TPP)Co^{II} diluted in a solid matrix of $TPPH_2$).[69] The latter complexes were analyzed with a simple first-order equation adopted from McGarvey,[83] which shows $g_{\perp} = 2.0023 + 6c_1$, with $c_1 = \lambda/\Delta E(xz,yz \rightarrow z^2)$. Thus, the absence of strong axial ligation along the z axis keeps the d_{z^2} orbital relatively low in energy and $\Delta E(xz,yz \rightarrow z^2)$ relatively small, which in turn leads to a large $g_{\perp}$ value. However, the presumed axially ligated [(MEC)Co^{II}(py)]$^-$ and [(PMC)Co^{II}(py)]$^-$ complexes still exhibit a large g_1 ($g_{||}$) value, with parameters that are quite similar to the four-coordinate species [(MEC)Co^{II}]$^-$ and [(PMC)Co^{II}]$^-$. These data suggest that the pyridine must bind very weakly to the cobalt center in these complexes, keeping $\Delta E(xz,yz \rightarrow z^2)$ small. These observations are in concert with a previous hypothesis from Hush and Woolsey that the negative charge of a Co^{II}−corrole complex prevented the binding of axial ligands through electronic repulsion,[84] in contrast to the strong binding seen for neutral cobalt(II) porphyrins and phthalocyanines.

From the EPR data it is clear that **3** binds pyridine much more tightly than the conventional Co^{II}−corroles. The difference in the affinity for axial ligands between cobalt(II) corroles versus corrolazines can be rationalized by the higher electronegativity of the *meso* N atoms in a corrolazine framework as compared to the *meso* carbon atoms of the conventional corroles. The *meso* N atoms make the cobalt center a stronger Lewis acid through electron-withdrawing effects. A similar argument has been used to explain the much tighter binding of pyridine to $(TBP)_8CzCo^{III}$ as compared to cobalt(III) corroles.[21] We made several attempts to produce a four-coordinate [(Cz)Co^{II}]$^-$ complex by reduction in noncoordinating solvents (toluene, CH_2Cl_2), but no EPR signal was observed, suggesting that the reduction does not take place under these conditions.

Binding of O_2. To our knowledge there are no reports describing the binding of O_2 to a Co^{II}−corrole, despite the large precedent that exists for such a reaction with Co^{II}−porphyrinoid and Schiff's base complexes.[35,36] Given that our Co^{II}−corrolazine complex exhibits EPR and pyridine binding properties similar to those of Co^{II}−porphyrins and corrins, it seemed reasonable to speculate that we might observe O_2 binding as well. Bubbling of O_2 through a freshly prepared solution of $[(TBP)_8CzCo^{II}(py)]^-$ in an EPR tube at −78 °C followed by rapid freezing in liquid nitrogen leads to the EPR spectrum shown in Figure 7. The EPR signal of $[(TBP)_8CzCo^{II}(py)]^-$ has disappeared and a spectrum attributable to a cobalt-dioxygen adduct is present. This spectrum has a much narrower spread in g values and smaller cobalt hyperfine interaction than the Co^{II} starting material, indicative of an organic radical-type EPR spectrum, as expected for a $Co^{III}-O_2^-$ species. A good simulation of this spectrum is also shown in Figure 7, and it was calculated by considering the **g** and **A** tensors noncoincident following the methods used for simulating numerous other (L)-$Co^{III}-O_2^-$ spectra (especially Jörin et al.,[42] as described in the Experimental Section). The g (1.996, 2.011, 2.075) and A (20, 40, 60 MHz) principal values obtained from the simulation match those of many other cobalt(III)−superoxo species.[35,36]

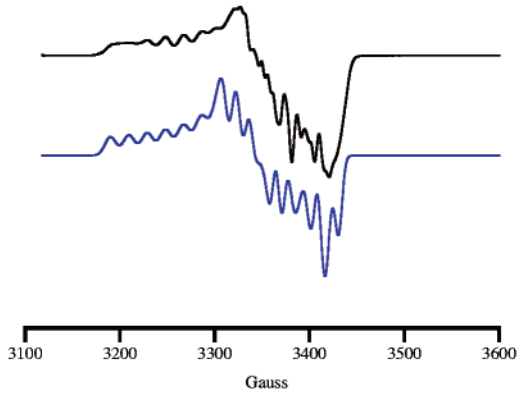

Figure 7. Experimental (black) and simulated (blue) EPR spectrum of $[(TBP)_8CzCo^{III}(py)(O_2)]^-$ in pyridine/EtOH (50/50 v/v) at 56 K. Experimental conditions: frequency, 9.477 GHz; incident microwave power, 4.66 mW; modulation frequency, 100 kHz; modulation amplitude, 1.0 G; receiver gain, 1.59×10^4. Simulation parameters: $\mathbf{g} = [1.996, 2.011, 2.075]$, $\mathbf{A}(^{59}Co) = [20.0, 40.0, 60.0]$ MHz; $\mathbf{A}(^{59}Co)$ rotated about **g** matrix by Euler angles: $\alpha = 15°$, $\beta = 25°$, $\gamma = 0$; a single-crystal Gaussian line width (hwhm) matrix, $\mathbf{W} = [12, 14, 20]$ MHz was also used.

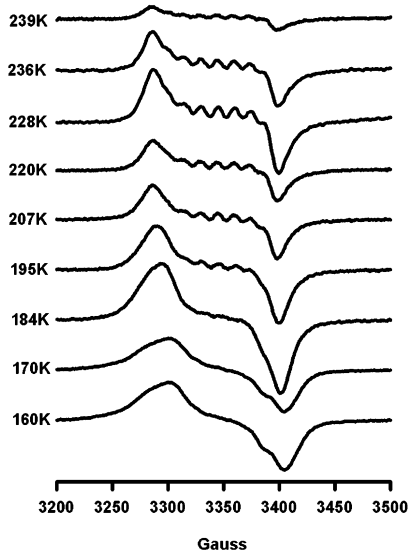

Figure 8. Variable-temperature EPR spectra of $[(TBP)_8CzCo^{III}(py)(O_2)]^-$ in fluid solution (pyridine/EtOH (50/50 v/v)). Temperature range from $T = 160$ to 239 K. Conditions: frequency, 9.464 GHz; incident microwave power, 0.938 mW; modulation frequency, 100.0 kHz; modulation amplitude, 10.0 G; receiver gain, 1.59×10^4.

Taken together, the overall features of the experimental spectrum and simulation lead to the conclusion that the reduced cobalt−corrolazine is capable of binding O_2 at low temperature to give a cobalt(III)−superoxo species.

Variable-Temperature Behavior of the Cobalt(III)−Superoxo Species. The overall stability and temperature-dependent O_2 binding characteristics of various $L_nCo^{III}O_2^-$ species have been of particular interest because of the importance in understanding the electronic and structural factors that control this process. Thus, the EPR spectrum of the cobalt−superoxo complex was measured at various temperatures from 160 to 239 K, as shown in Figure 8. At temperatures above ∼200 K, a clear eight-line pattern is obtained, and the experimental spectrum at 228 K has been simulated to give $A_{iso}(^{59}Co) = 40$ MHz and $g_{iso} = 2.026$. Note that these values are an exact average of the individual $\mathbf{A}(^{59}Co)$ and **g** components seen in frozen solution (Figure 7), confirming the retention of the

superoxo complex in fluid solution. Similar spectra and simulations have been obtained for a number of $L_nCo^{III}O_2^-$ complexes in isotropic media.[88−92] The EPR spectrum disappears at $T >$ 240 K, indicative of a shift to the right in the equilibrium $L_nCo^{III}O_2^- \leftrightarrows (L_n)Co^{II} + O_2$. A shift of this type is typical of a cobalt−dioxygen adduct. Thawing and refreezing of the oxygenated sample can be cycled several times before decay of the sample occurs. We speculate that the binding of O_2 is successful in the case of a triazacorrole and not the conventional corroles because of two main reasons: the d_{z^2} ground state exhibited by the cobalt(II)−triazacorrole is essential for O_2 coordination, and the *meso* N atoms are electron-withdrawing compared to carbon, which helps to stabilize the overall anionic charge of the $CzCo^{II}$ unit and favor binding of O_2.

Generation of Free Superoxide Anion. Interestingly, an EPR spectrum for free superoxide anion can be observed if the Co^{II} solution is exposed to a large excess of dioxygen. If the solution of $[(TBP)_8CzCo^{II}(py)]^-$ is bubbled with oxygen for greater than ∼30 s at room temperature and then frozen to 77 K, neither the EPR spectrum of the Co^{II} complex nor that of the $Co^{III}-O_2^-$ is seen, but rather a new spectrum which corresponds to free superoxide anion is observed $\mathbf{g} =$ [2.10, 2.00, 1.98]. A separate sample of KO_2 was dissolved in the same solvent mixture (pyridine/EtOH 50/50) and revealed an identical EPR spectrum at 77 K. There are a few well-documented examples of the production of free O_2^- by similar metal complexes; Co^{II}−tetrasulfophthalocyanine was shown to release O_2^- in the presence of CN^- or OH^-,[93] and the porphyrin complexes (OEP)RhCl[94] and (TPP)Co[95] have been shown to generate free O_2^- via a putative, short-lived $M^{III}-O_2^-$ intermediate. It is unclear at this time why further oxygenation of $[(TBP)_8CzCo^{II}(py)]^-$ causes the release of superoxide, but these results demonstrate that free O_2^- is easily detectable by EPR under our conditions and support our previous conclusion that $[(TBP)_8CzCo^{II}(py)]^-$ exhibits reversible O_2 binding behavior under relatively low concentrations of O_2.

Conclusions

We have synthesized two new cobalt corrolazine complexes bearing the isoelectronic, σ-bonded axial ligands CN^- and $C{\equiv}CSiPh_3^-$. These complexes are rare examples of formally high oxidation state cobalt corroles. From a combination of synthetic observations, FTIR, EPR, SQUID, UV−vis, and in the case of the acetylide complex X-ray crystallography, we suggest their electronic configurations are best formulated as $(Cz^{+\bullet})Co^{III}(CN)$ and $(Cz)Co^{IV}(CCSiPh)_3 \leftrightarrow (Cz^{+\bullet})Co^{III}(CCSiPh)_3$, respectively. Thus, in both cases it appears as though there is significant "noninnocent" character to the corrolazine ligand, although more detailed spectroscopic work (e.g. ESEEM/ENDOR studies[46]) is needed to make quantitative spin density assignments for the corrolazine ligand versus the cobalt metal ion. We have also generated the reduced cobalt(II) complex $[(TBP)_8(CzCo^{II}(py)]^-$ and have shown that it has a typical low-spin Co^{II} d_{z^2} ground state by EPR spectroscopy, in contrast to the few earlier examples of cobalt(II) corroles. In addition, we have demonstrated that the cobalt(II) complex will reversibly bind dioxygen, which is a reaction well established in porphyrin chemistry but previously unknown for cobalt corroles. The oxygen adduct was characterized by EPR spectroscopy as a typical cobalt(III)−superoxo adduct, and shown to be stable at temperatures below ∼240 K by VT-EPR measurements.

Acknowledgment. This work was supported by the NSF (Grants CHE0094095 and CHE0089168 to D.P.G., CHE0091968 to A.L.R.). D.P.G. is also grateful for an Alfred P. Sloan Research Fellowship (B.R.-4153). A.C. is grateful for the Italian MIUR fund.

Supporting Information Available: X-ray crystallographic file for compound **2** (CIF). This material is available free of charge via the Internet at http://pubs.acs.org.

JA036983S

(88) Hoffman, B. M.; Diemente, D. L.; Basolo, F. *J. Am. Chem. Soc.* **1970**, *92*, 61−65.
(89) Hoffman, B. M.; Petering, D. H. *Proc. Natl. Acad. Sci. U.S.A.* **1970**, *67*, 637−643.
(90) Walker, F. A.; Bowen, J. *J. Am. Chem. Soc.* **1985**, *107*, 7632−7635.
(91) Bowen, J. H.; Shokhirev, N. V.; Raitsimring, A. M.; Buttlaire, D. H.; Walker, F. A. *J. Phys. Chem. B.* **1997**, *101*, 8683−8691.
(92) Van Doorslaer, S.; Schweiger, A.; Kräutler, B. *J. Phys. Chem. B.* **2001**, *105*, 7554−7563.
(93) Wagnerová, D. M.; Lang, K.; Damerau, W. *Inorg. Chim. Acta* **1989**, *162*, 1−3.
(94) Sakurai, H.; Uchikubo, H.; Ishizu, K.; Tajima, K.; Aoyama, Y.; Ogoshi, H. *Inorg. Chem.* **1988**, *27*, 2691−2695.
(95) Sakurai, H.; Ishizu, K. *J. Am. Chem. Soc.* **1982**, *104*, 4960−4962.